

Transformation of stishovite to a denser phase at lower-mantle pressures

Kathleen J. Kingma, Ronald E. Cohen,
Russell J. Hemley & Ho-kwang Mao

Geophysical Laboratory and Center for High-Pressure Research,
Carnegie Institution of Washington, 5251 Broad Branch Road, N.W.,
Washington DC 20015, USA

WHETHER stishovite, the highest-pressure polymorph of SiO_2 known from natural samples, transforms to a denser structure at higher pressures has long been of interest. A suggested transition from rutile to the CaCl_2 structure driven by a vibrational-mode instability¹ was supported by the observation of a frequency decrease (softening) of a Raman mode with increasing pressure². Subsequent X-ray diffraction measurements provided evidence³ for stability of the CaCl_2 phase near 100 GPa. Electronic-structure calculations predict, however, that the transition occurs at much lower pressure, where a shear modulus vanishes and before the Raman mode softens completely⁴. Here we use *in situ* Raman spectroscopy and a new theoretical model to investigate the high-pressure behaviour of stishovite. At 50 GPa, the pressure dependence of the soft B_{1g} mode abruptly changes and the E_g mode splits, as predicted for transformation to the CaCl_2 structure. Our results demonstrate that any free silica in the deep mantle (below 1,200–1,500 km) will exist in the CaCl_2 structure at considerably lower pressures than previously thought³.

Study of stishovite under mantle conditions has been difficult. The bulk modulus of stishovite, although now well constrained from single-crystal Brillouin scattering⁵, has been controversial, with values varying significantly between static compression diffraction studies^{3,6–9}. These discrepancies arise because compression of stishovite is highly anisotropic and sensitive to non-hydrostatic stress conditions. Although *in situ* X-ray diffraction data suggested that silica was stable in the CaCl_2 structure above ~ 100 GPa (ref. 3) the nonhydrostatic conditions of these experiments precluded the unambiguous determination of the transition pressure. Because the atomic displacements from the rutile to the CaCl_2 structure are subtle, and the volume change at the transition is likely to be small⁴, diffraction methods may not detect the onset and initial stages of this transformation. The vibrational spectrum is an important diagnostic of mineral structure and is complementary to diffraction techniques¹⁰. Spectroscopic measurements for stishovite^{2,11–15} date back to the mineral's discovery^{16,17}. Controversy surrounded the Raman spectrum of stishovite because of its very low scattering cross-section and problems with sample purity (see ref. 14). This was resolved with the development of new techniques^{2,14}, advances which also permitted measurement of the Raman spectrum to 32 GPa. The observed softening of the B_{1g} mode suggested² a transition below 100 GPa.

A number of theoretical calculations of post-stishovite phases have been performed, including simple ionic models, molecular-cluster methods, and crystalline electronic-structure computations (see ref. 18 for review). Ionic-model calculations have predicted a range of rutile-to- CaCl_2 transition pressures for silica, mostly above 100 GPa. Recently, however, calculations using the linear-augmented plane-wave (LAPW) method predicted the transition should occur at 45 GPa where the C_{11} - C_{12} elastic shear modulus vanishes⁴. These calculations employed the local density approximation (LDA) for the quantum-mechanical exchange and correlation interactions; no experimental data were used. According to the LAPW results, the soft rutile B_{1g} mode should become a hard mode of A_g symmetry at the transition. This shows that the rutile-to- CaCl_2 transition in silica

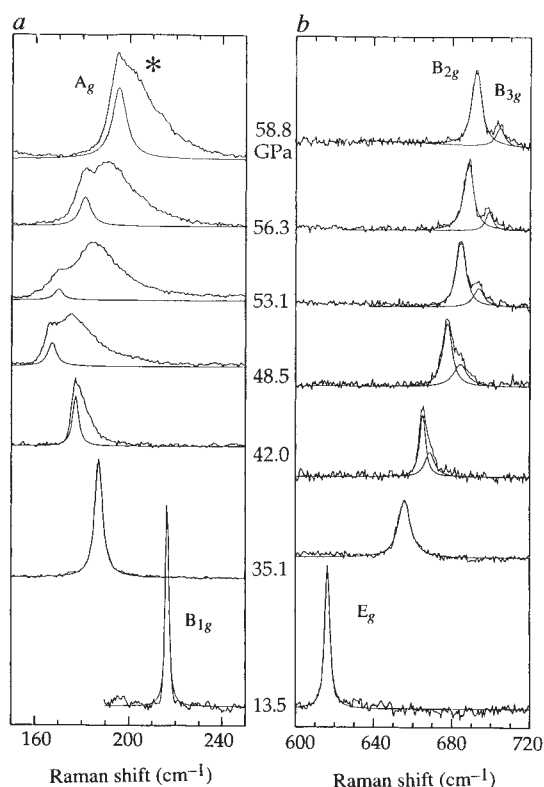


FIG. 1 Representative Raman spectra showing evidence for the rutile-to- CaCl_2 transition in silica. Lorentzian fits to the bands predicted by theory are shown as smooth traces. *a*, Initial frequency decrease (softening) of the rutile B_{1g} mode with pressure followed by frequency increase (hardening) of the CaCl_2 A_g mode with which the rutile B_{1g} is correlated. A broad band which is not predicted by theory was observed above 40 GPa (marked by asterisk in topmost panel). The new broad band is highly dependent on stress conditions; in our nonhydrostatic experiments, a broad feature was observed to split from the rutile B_{1g} band at ~ 20 GPa. Similar asymmetric broadening of the B_{1g} fundamental was noticed at the highest pressures of the previous experiment² which used the argon pressure medium (less hydrostatic than neon). This may arise from stress at grain-grain interfaces or at boundaries of twin domains which form at the transition, or from a further reduction in symmetry (possibly associated with residual stress inhomogeneities). Low-frequency, broad bands associated with multiphonon scattering are also observed²⁹ in α -quartz-structured SiO_2 and AlPO_4 . *b*, Splitting of the rutile E_g mode into the CaCl_2 B_{2g} and B_{3g} modes. All measurements were made at room temperature (298 K) using a Dilor XY spectrometer equipped with a modified optical microscope, custom-built confocal imaging optics, and a liquid-nitrogen-cooled CCD (charge-coupled device) detector. An argon-ion laser was used as the excitation source; 488.0- and 514.5-nm lines were used to check for Raman activity of observed bands. The laser radiation was focused to sample areas $< 5 \mu\text{m}$ in diameter. Pressures were determined with the ruby-fluorescence method (quasi-hydrostatic scale)³⁰. With neon as the medium, pressure gradients never exceeded 0.5 GPa.

should have a characteristic, and indeed unusual, signature in the high-pressure Raman spectrum. Motivated by the excellent agreement between the calculated⁴ and experimentally observed² mode behaviour, we have investigated the vibrational properties of stishovite using new Raman scattering techniques to test this theoretical prediction. Factor-group analysis also shows that the rutile E_g should split into B_{2g} and B_{3g} modes at the transition.

Experiments were performed using a Mao-Bell diamond-anvil cell¹⁹. Type I diamonds with very low fluorescence were used to limit the background signal. Starting materials for all experiments were synthesized in a multi-anvil press from natural

TABLE 1 Frequencies and pressure shifts of observed Raman-active bands*

Stishovite (1 bar)			CaCl ₂ -structured SiO ₂ (50 GPa)			
Symmetry [†]	ν_i (cm ⁻¹)	$(d\nu_i/dP)_T$ (cm ⁻¹ GPa ⁻¹)	Correlation [‡]	Symmetry [†]	ν_i (cm ⁻¹)	$(d\nu_i/dP)_T$ (cm ⁻¹ GPa ⁻¹)
B _{2g}	966.2 (5)	3.68 (6)	→	B _{1g}	(Not observed)	
A _{1g}	754.1 (3)	3.12 (7)		A _g	906	2.2 (2)
E _g	589 (1)	2.09 (2)		B _{2g}	684	0.99 (8)
				B _{3g}	706	2.1 (2)
				Broad band	177	3.3 (2)
B _{1g}	231.6 (3)	-0.93 (2)	→	A _g	163	3.2 (2)

* Frequencies (ν_i), and isothermal pressure shifts ($d\nu_i/dP$) for the observed Raman-active bands of stishovite at 1 bar and CaCl₂-structured SiO₂ at 50 GPa (298 K).

[†] Irreducible representations for the zone-centre optical modes of vibration, Γ_{op} , are calculated for the rutile and CaCl₂ structures by factor-group analysis. Rutile ($P4_2/mnm, D_{4h}^{14}$), $\Gamma_{op} = A_{1g}^R + A_{2g}^R + A_{2u}^R + B_{1g}^R + B_{2g}^R + 2B_{1u}^R + E_g^R + 3E_u^R$, CaCl₂ ($Pnmm, D_{2h}^{12}$), $\Gamma_{op} = 2A_g^R + 2A_u + 2B_{1g}^R + B_{2g}^R + B_{3g}^R + B_{1u}^R + 3B_{2u}^R + 3B_{3u}^R$. Here superscript 'R' denotes Raman-active modes, superscript 'IR' denotes infrared-active modes, and the unmarked modes are neither Raman- nor infrared-active. The symbols A, B and E indicate the vibrational symmetry, where A and B denote one-dimensional, and E two-dimensional modes. Subscript *g* indicates vibrations which are symmetric with respect to a centre of inversion, and subscript *u* indicates those which are antisymmetric with respect to inversion.

[‡] In correlating modes, $a_{1(rutile)} = a_{(CaCl_2)}$, $a_{2(rutile)} = b_{(CaCl_2)}$ and $c_{(rutile)} = c_{(CaCl_2)}$, where *a*, *b* and *c* are lattice parameters.

quartz. Care was taken to avoid contamination that complicated other studies^{13,14}. Because hydrostatic conditions were essential, stishovite grains (1–5 μm) were compressed using neon as the pressure-transmitting medium; neon remains nearly hydrostatic (quasi-hydrostatic) to significantly higher pressure²⁰ than media used in previous work (for example, no medium³, salt¹⁵ and argon²). Stishovite powder was also compressed without a medium to examine nonhydrostatic effects.

During quasi-hydrostatic compression of stishovite, each of the four Raman-active modes predicted for the rutile structure were observed; pressure shifts (Table 1) are consistent with results of the earlier lower-pressure study². At 40 GPa, the stishovite B_{1g} mode showed significant asymmetry, and by 50 GPa two peaks could be resolved (Fig. 1)—a sharp peak that lies along the trend of the negative pressure shift of the stishovite B_{1g} and a broad band centred $\sim 15 \text{ cm}^{-1}$ higher in frequency than the sharp B_{1g}. With further compression, the pressure shift of both bands suddenly changed, becoming positive (Fig. 2). The stishovite E_g mode was asymmetric by 40 GPa, and two peaks were clearly resolved above 50 GPa (Fig. 1). A slight break in the slope of the pressure shift of the strong stishovite A_{1g} mode

was observed at 50 GPa (Fig. 3), and the pressure dependence of the weak high-frequency stishovite B_{2g}, which was not observed previously under compression², could be determined (Table 1). This band was lost above 48 GPa because of its weakness and the increase in background signal with increasing pressure. All changes were reversible, and no hysteresis could be detected on decompression (Fig. 2).

The abrupt change in the pressure-dependence shift of the lowest-frequency mode occurs at a pressure of $50(\pm 3)$ GPa; the uncertainty arises from fitting the overlapping low-frequency peaks (Fig. 1). The Raman results reported here are in remarkable agreement with the earlier LAPW calculations⁴ and demonstrate that stishovite transforms to the CaCl₂ structure on quasi-hydrostatic compression—not only is the transition pressure closely predicted, but the calculated behaviour of the modes is accurate (Fig. 3). At pressures above the phase transition, four sharp bands and one broad band are observed in the Raman spectrum (Table 1, Fig. 3). Mode assignments for the sharp bands of the high-pressure polymorph were easily made by analogy with similar CaCl₂-structured compounds²¹. The origin of the broad, low-frequency band is discussed in the legends of Figs

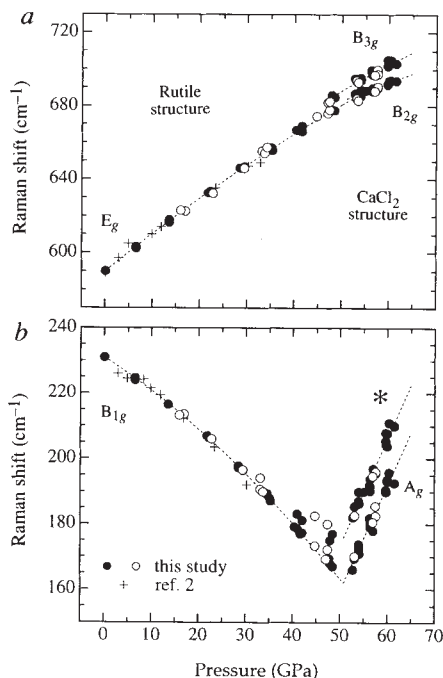


FIG. 2 Frequency shifts of the mid-frequency (a) and low-frequency (b) Raman bands during compression (filled circles) and decompression (empty circles) through the rutile-to-CaCl₂ transition in silica. The dashed curves are quadratic fits of the data plotted to guide the eye. The frequency shift of the new broad band (marked with asterisk) is found to parallel the frequency shift of the CaCl₂ A_g mode. Results at lower pressure are in excellent agreement with those reported in ref. 2.

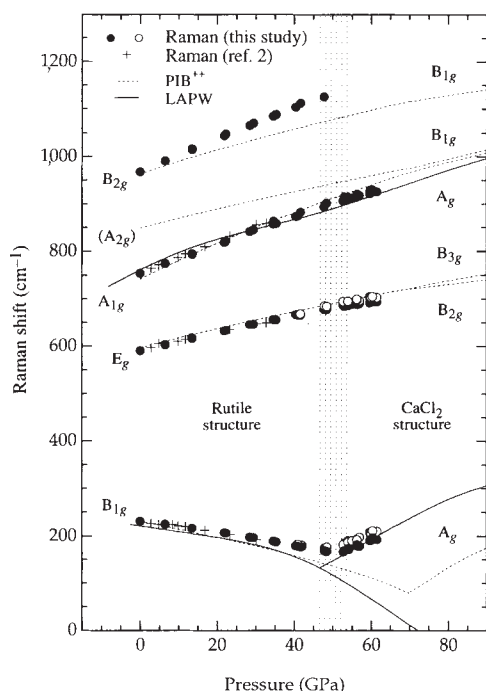


FIG. 3 Comparison of experimental frequency shifts during compression with theoretical LAPW⁴ and PIB⁺⁺ calculations (see text). The experimentally determined pressure for the rutile-to-CaCl₂ transition in silica from this work is shown as the stippled vertical band. LAPW results constraining the symmetry to remain that of stishovite appear as extension of the rutile B_{1g} frequency shift curve at pressures above the transition. The general mode behaviour is reproduced well by the new PIB⁺⁺ model; the frequency shifts of the rutile B_{2g} mode and especially the rutile E_g, which were not calculated in the LAPW study, are in good agreement with the Raman measurements, especially considering that there is no fit to experimental data. The PIB⁺⁺ model predicts that the Raman-active CaCl₂ B_{1g} mode that correlates with the silent (non-active) A_{2g} mode in stishovite is almost degenerate with the high-frequency CaCl₂ A_g mode. Thus it is likely that this CaCl₂ B_{1g} mode was hidden in the Raman measurements by the strong CaCl₂ A_g mode. Additionally, the PIB⁺⁺ results demonstrate that the new, broad feature observed at low frequency (Figs 1 and 2) cannot be either of the unobserved CaCl₂ B_{3g} modes, which should occur above 900 cm⁻¹. The transition pressure, which is very sensitive to the details of the potential, is over-estimated by 20 GPa by the PIB⁺⁺ calculations. Although this model uses the LDA and is non-empirical, the potential is parametrized and fitted to the LAPW total energies, and thus is less reliable than the electronic-structure calculations themselves. The observed flattening of the pressure dependence of the rutile B_{1g} mode and CaCl₂ low-frequency A_g mode relative to the zero-temperature LAPW calculations near the transition is probably due to anharmonicity, which was not included in the first-principles calculation.

1 and 3. The excellent agreement between theory and experiment demonstrates the power of new electronic-structure methods; this may be one of the best examples of an accurate first-principles prediction of a phase transition.

A pressure of 50 GPa corresponds to a depth in the Earth of ~1,200 km. The temperature^{22,23} of the mantle at this depth ranges from 2,000 to 2,500 K. We examined the temperature dependence of the transition in silica and also confirmed mode assignments using a new non-empirical lattice dynamical model (PIB⁺⁺)¹⁸, which is based on the potential induced breathing (PIB) model but is fitted to the results of the earlier LAPW frozen-phonon calculations⁴. Results at ambient temperature are shown in Fig. 3. Most importantly, the PIB⁺⁺ calculations predict a small temperature dependence for the transition of ~250 K GPa⁻¹, so that any free silica in the lower mantle would transform to the CaCl₂ structure at ~60 GPa assuming an upper temperature bound of 2,500 K.

Thermoelastic data indicate a high perovskite abundance in the lower mantle, and possible enrichment of silica and/or iron relative to the upper mantle^{22,23}. The existence of a stable silica phase with free energy lower than that of stishovite drives the reaction (Mg, Fe)SiO₃ perovskite → (Mg, Fe)O magnesio-wüstite + SiO₂. Additionally, if iron enrichment is significant,

the production of magnesio-wüstite and a silica phase is further promoted by the inability of perovskite to accommodate large amounts of iron²³.

We have shown that the rutile-to-CaCl₂ transition occurs in silica at lower-mantle pressures. Because an elastic instability is associated with the transition, a shear modulus is anomalously soft near the phase change. Free silica in the lower mantle may therefore lead to an observable seismic discontinuity around a depth of 1,200–1,500 km. Although globally recognized discontinuities have been restricted to the upper mantle (<660 km), there are reports of local discontinuities which cluster in the range of the new transition pressure^{24–26}. Thus although present seismological observations seem to preclude global discontinuities in the lower mantle²⁷, new techniques allowing for mapping at much higher resolutions should be employed to look for the seismic signal of the stishovite transformation. Such a signal, or lack thereof, would place limits on the amount of free silica in the lower mantle. Moreover, the new transition is geophysically important for experimentally documented reactions involving the production of free silica from iron and perovskite which may be associated with the anomalous seismic structure in D'', the 100- to 300-km region at the base of the mantle²⁸. □

Received 2 November 1994; accepted 17 January 1995.

- Nagel, L. & O'Keefe, M. *Mater. Res. Bull.* **6**, 1317–1320 (1971).
- Hemley, R. J. in *High-Pressure Research in Mineral Physics* (eds Manghni, M. H. & Syono, Y.) 347–359 (Terra Scientific, Tokyo and Am. Geophys. Union, Washington DC, 1987).
- Tsuchida, Y. & Yagi, T. *Nature* **340**, 217–220 (1989).
- Cohen, R. E. in *High-Pressure Research: Application to Earth and Planetary Sciences* (eds Syono, Y. & Manghni, M. H.) 425–431 (Terra Scientific, Tokyo and Am. Geophys. Union, Washington DC, 1992).
- Weidner, D. J., Bass, J. D., Ringwood, A. E. & Sinclair, W. J. *geophys. Res.* **87**, 4740–4746 (1982).
- Liu, L. G., Bassett, W. A. & Takahashi, T. *J. geophys. Res.* **79**, 1160–1164 (1974).
- Sato, Y. *Earth planet. Sci. Lett.* **34**, 307–312 (1977).
- Sugiyama, M., Endo, S. & Koto, K. *Miner. J.* **13**, 455–466 (1987).
- Ross, N. L., Shu, J.-F. & Hazen, R. M. *Am. Miner.* **75**, 739–747 (1990).
- McMillan, P. F. & Hofmeister, A. M. in *Spectroscopic Methods in Mineralogy and Geology* (ed. Hawthorne, F. C.) 99–159 (Mineralogical Soc. Am., Washington DC, 1988).
- Lyons, R. J. *Nature* **196**, 266–267 (1962).
- Kieffer, S. W. *Rev. Geophys. Space Phys.* **17**, 20–33 (1979).
- Hofmeister, A. M., Xu, J. & Akimoto, S. *Am. Miner.* **75**, 951–955 (1990).
- Hemley, R. J., Mao, H. K. & Chao, E. C. T. *Phys. Chem. Miner.* **13**, 285–295 (1986).

- Williams, Q., Hemley, R. J., Kruger, M. B. & Jeanloz, R. J. *geophys. Res.* **98**, 22157–22170 (1993).
- Stishov, S. M. & Popova, S. V. *Chemistry (USSR)* **10**, 923–926 (1961).
- Chao, E. C. T., Fahey, J. J., Littler, J. & Milton, D. J. *J. geophys. Res.* **67**, 419–421 (1962).
- Cohen, R. E. in *Silica: Physical Behavior, Geochemistry and Materials Applications* (eds Heaney, P. J., Prewitt, C. T. & Gibbs, G. V.) 369–402 (Reviews in Mineralogy, Vol. 29, Mineralogical Soc. Am., Washington DC, 1994).
- Mao, H. K. & Bell, P. M. *Yb. Carnegie Instn Wash.* **77**, 904–908 (1978).
- Bell, P. B. & Mao, H. K. *Yb. Carnegie Instn Wash.* **80**, 404–406 (1981).
- Weber, W. H., Graham, G. W. & McBride, J. R. *Phys. Rev.* **B42**, 10969–10975 (1990).
- Knittle, E., Jeanloz, R. & Smith, G. L. *Nature* **319**, 214–216 (1986).
- Stixrude, L., Hemley, R. J., Fei, Y. & Mao, H. K. *Science* **257**, 1099–1101 (1992).
- Johnson, L. R. *Bull. seism. Soc. Am.* **59**, 973–1008 (1969).
- Vinnik, L. P., Lukk, A. A. & Nikolaev, A. V. *Phys. Earth planet. Inter.* **5**, 328–331 (1972).
- Wicks, C. W. *EOS (abstr.)* **74**, 550 (1993).
- Dziewonski, A. M. & Anderson, D. L. *Phys. Earth planet. Inter.* **22**, 277–288 (1981).
- Knittle, E. & Jeanloz, R. *Science* **251**, 1438–1443 (1991).
- Jayaraman, A., Wood, D. L. & Maines, R. G. *Sr Phys. Rev.* **B35**, 8316–8321 (1987).
- Mao, H. K., Xu, J. & Bell, P. M. *J. geophys. Res.* **91**, 4673–4676 (1986).

ACKNOWLEDGEMENTS. We thank Y. Fei and M. Walter for synthesis of starting samples. This research was supported by the US NSF, including support to D. Veblen at the Department of Earth and Planetary Sciences of The Johns Hopkins University.